Vol. 11 No. 4 PROGRESS IN NATURAL SCIENCE April 2001

Inversion method for defects in depth evaluation and thermal wave imaging*

LÜ Yuekai (吕跃凯), ZHANG Shuyi (张淑仪) and ZHOU Qingbiao (周庆标)

Laboratory of Modern Acoustics, Institute of Acoustics, Nanjing University, Nanjing 210093, China

Received June 12, 2000; revised July 19, 2000

Abstract A hybrid Newton-like iterative method and a regularization method are employed to perform the numerical simulations of the defects in depth evaluation and the thermal wave imaging for defects-included solid sample by analysis of the surface photo-thermal signals. A simple and effective data processing method is suggested to improve the reconstructed data. The results of the numerical calculation demonstrate that the algorithm presented in this paper is very effective, and can be used for qualitative and quantitative analyses of homogeneous materials with defects in depth included. It is also proved that the algorithm is stable even with noise disturbance.

Keywords: **depth reconstruction, defect in depth evaluation, thermal wave imaging.**

Thermal wave imaging has become a powerful technique for non-destructive evaluation. It is being used in aerospace exploration, automobile and military industries, and also in medical diagnoses, etc.[1~4]. In this paper, we employ an inversion method to perform the numerical simulation of the thermal wave imaging for defects-included homogeneous samples using the surface photo-thermal signals. The idea is to generate a thermal wave in the investigated sample by means of a periodically intensity-modulated laser of frequency ω. The propagating thermal wave in the sample is partially scattered back due to the changes of the thermal properties and eventually detected at the sample's surface. As we know, the modulation frequency ω determines the penetration depth of the thermal wave in the investigated sample. Therefore, by adjusting the frequency in a sufficiently wide range, one can obtain a set of detected data corresponding to different frequencies. The data contain the information about the thermal properties of the sample, which can be used for thermal wave imaging and defects in depth evaluation by utilizing the inversion method.

The numerical simulation involves three steps. Firstly, solve the heat conduction equation in the frequency domain for homogeneous samples to calculate the surface temperature with a set of modulation frequencies, which can be assumed as the detected surface signals. To confirm the reliability of the algorithm of inversion, the simulated surface signals can be mingled with deliberate noises. Secondly, employ the pulse spectrum technique (PST) and a regularization method[5] to reconstruct the depth profile of the thermal conductivity $\kappa(z)$ of the investigated sample (inverse problem). Thirdly, establish a simple and effective data processing method to improve the reconstructed data. From the improved data, the desired information about defects in the sample can be precisely

* Project supported by the National Natural Science Foundation of China (Grant No. 19634050).

determined and the thermal images of the sample can also be obtained.

1 Inversion algorithm

We consider a thermally opaque solid sample with thickness L, and assume that the sample is irradiated by a periodically intensity-modulated pumping laser with frequency ω. The light energy is absorbed at the surface only, and the heat flow from the sample into the surroundings can be neglected. For the considered sample, the thermal conduction equation in the frequency domain is

$$\frac{\mathrm{d}}{\mathrm{d}z}\left[\kappa(z)\frac{\mathrm{d}T(z,\omega)}{\mathrm{d}z}\right]-i\omega\rho(z)c(z)T(z,\omega)=0,\qquad(0\leqslant z\leqslant L)\tag{1a}$$

with the boundary conditions at $z=0$ and L

$$-\kappa(0)\frac{\mathrm{d}T(z,\omega)}{\mathrm{d}z}\bigg|_{z=0}=g(\omega),\tag{1b}$$

$$-\kappa(L)\frac{\mathrm{d}T(\omega,t)}{\mathrm{d}z}\bigg|_{z=L}=0,\tag{1c}$$

where $T(z,\omega)$ is the Fourier transform of the time-dependent temperature $T(z,t)$, $g(\omega)$ the Fourier transform of the surface heat flux $g(t)$; and $\kappa(z)$, $\rho(z)$ and $c(z)$ are the thermal conductivity, density, and specific heat of the sample respectively. In the photo-thermal experiments, the surface temperature $T_d(\omega)$ can be detected at a series of frequencies $\{\omega_i\}$

$$T(0,\omega_i)=T_d(\omega_i),\qquad(i=1,2,\cdots,M).\tag{2}$$

The inversion problem is to determine the distributions of the thermal parameters using Formulas (1a) ~ (1b) in terms of the detected surface signals (2). For simplicity, we assume that the ρc is constant, and only the reconstruction of $\kappa(z)$ is considered. Because the evaluated object is a defects-included homogeneous medium, the thermal conductivity $\kappa(z)$ is expected to be a step function. By employing the pulsed spectrum technique (PST)[6], an iterative method for the reconstruction of depth profile of $\kappa(z)$ from the photo-thermal data can be established. Firstly, one guesses an initial value for the unknown functions $\kappa(z)$, and then constructs a Newton-like iterative process

$$T^{l+1}(z,\omega)=T^{l}(z,\omega)+\delta T^{l}(z,\omega),\tag{3a}$$

$$\kappa^{l+1}(z)=\kappa^{l}(z)+\delta\kappa^{l}(z).\tag{3b}$$

Substituting the iterative Eqs. (3a) ~ (3b) to Eqs. (1a) ~ (1c) and neglecting the higher order terms of $\delta T^{l}(z,\omega)$ and $\delta\kappa^{l}(z)$, one can get the following iterative equations for determination of $T^{l}(z,\omega)$:

$$\frac{\mathrm{d}}{\mathrm{d}z}\left[\kappa^{l}(z)\frac{\mathrm{d}T^{l}(z,\omega)}{\mathrm{d}z}\right]-i\omega\rho cT^{l}(z,\omega)=0,\tag{4a}$$

$$\kappa^l(0)\frac{\mathrm{d}T^l(z,\omega)}{\mathrm{d}z}\bigg|_{z=0} = -g(\omega), \tag{4b}$$

$$\kappa^l(L)\frac{\mathrm{d}T^l(z,\omega)}{\mathrm{d}z}\bigg|_{z=L} = 0, \tag{4c}$$

and the equations for $\delta T^l(z,\omega)$,

$$\frac{\mathrm{d}}{\mathrm{d}z}\left\{\kappa^l(z)\frac{\mathrm{d}\delta T^l(z,\omega)}{\mathrm{d}z}\right\} - i\omega\rho c\delta T^l(z,\omega) = -\frac{\mathrm{d}}{\mathrm{d}z}\left[\delta\kappa^l(z)\frac{\mathrm{d}T^l(z,\omega)}{\mathrm{d}z}\right], \tag{5a}$$

$$\kappa^l(0)\frac{\mathrm{d}\delta T^l(z,\omega)}{\mathrm{d}z}\bigg|_{z=0} = -\delta\tau^l(0)\frac{\mathrm{d}T^l(z,\omega)}{\mathrm{d}z}\bigg|_{z=0}, \tag{5b}$$

$$\kappa^l(L)\frac{\mathrm{d}\delta T^l(z,\omega)}{\mathrm{d}z}\bigg|_{z=L} = -\delta\kappa^l(L)\frac{\mathrm{d}T^l(z,\omega)}{\mathrm{d}z}\bigg|_{z=L}. \tag{5c}$$

By $T^l(z,\omega)\times 4(\mathrm{a}) - \delta T^l(z,\omega)\times 5(\mathrm{a})$ and then using Green theorem, one can obtain a Fredholm integral equation of the first kind to determine $\delta\kappa^l(z)$ as follows:

$$\int_0^L \delta\kappa^l(z)\left[\frac{\mathrm{d}T^l(z,\omega)}{\mathrm{d}z}\right]^2\mathrm{d}z = g(\omega)\left[T^l(0,\omega) - T_d(\omega)\right], \tag{6}$$

where $T_d(\omega)$ is the surface temperature that can be detected at frequencies $\{\omega_j\}$ in photo-thermal experiments. The right-hand side of Eq. (6) can be obtained using the approximation

$$\delta T^l(0,\omega) \cong T_d(\omega) - T^l(0,\omega). \tag{7}$$

Now the inverse problem of the depth distribution of $\kappa(z)$ is translated to the determination of $\delta\kappa^l(z)$ from the integral Eq. (6). To do this, we can turn Eq. (6) into discrete algebraic equations and then using the method of singular value decomposition (SVD) to construct a least square solution. Expanding $\delta\tau^l(z)$ by a normalized and orthogonal function set $\{\phi_k(z),\ k=1,2,\cdots,N\}$,

$$\delta\kappa^l(z) = \sum_{k=1}^{N} b_k\phi_k(z), \tag{8}$$

and taking frequencies $\{\omega_j,\ j=1,2,\cdots,M\}$, one can get a set of $M\times N$ of linear algebraic equations

$$\boldsymbol{A}_c\boldsymbol{B} = \boldsymbol{D}_c, \tag{9}$$

where $\boldsymbol{A}_c$ is an $M\times N$ complex coefficient matrix with elements a_{jk}

$$a_{jk} = \int_0^L\left[\frac{\mathrm{d}T^l(z,\omega_j)}{\mathrm{d}z}\right]^2\phi_k(z)\mathrm{d}z, \qquad (j=1,2,\cdots,M,\ k=1,2\cdots,N), \tag{10}$$

and $\boldsymbol{D}_c$ is a complex column vector relating the detecting surface data with elements

$$d_j = g(\omega_j)[T^l(0,\omega_j) - T_d(\omega_j)], \qquad (j = 1,2,\cdots,M). \tag{11}$$

It must be pointed out that matrix equation (9) is a set of complex coefficient algebraic equations, but $\delta\kappa^l(z)$ must be real for each iteration, so the column vector $\boldsymbol{B}$ to be determined must be a real column vector. By separating the real and imaginary parts of Eq. (9), a set of $2M \times N$ of real coefficient linear algebraic equations can be obtained

$$\boldsymbol{A}_{\mathrm{r}}\boldsymbol{B} = \boldsymbol{D}_{\mathrm{r}}, \tag{12}$$

where the $2M \times N$ real matrix $\boldsymbol{A}_{\mathrm{r}}$ and the $2M$ real column vector $\boldsymbol{D}_{\mathrm{r}}$ take the forms

$$\boldsymbol{A}_{\mathrm{r}} = \begin{pmatrix} \boldsymbol{A}_{\mathrm{c}}^{\mathrm{r}} \\ \boldsymbol{A}_{\mathrm{c}}^{\mathrm{i}} \end{pmatrix}, \qquad \boldsymbol{D}_{\mathrm{r}} = \begin{pmatrix} \boldsymbol{D}_{\mathrm{c}}^{\mathrm{r}} \\ \boldsymbol{D}_{\mathrm{c}}^{\mathrm{i}} \end{pmatrix}, \tag{13}$$

in which, $\boldsymbol{A}_{\mathrm{c}}^{\mathrm{r}}$ and $\boldsymbol{A}_{\mathrm{c}}^{\mathrm{i}}$ (or $\boldsymbol{D}_{\mathrm{c}}^{\mathrm{r}}$ and $\boldsymbol{D}_{\mathrm{c}}^{\mathrm{i}}$) are the real part and the imaginary part of $\boldsymbol{A}_{\mathrm{c}}$ (or $\boldsymbol{D}_{\mathrm{c}}$), respectively. In the experiment, a finite series of experimental data can be obtained, and the total number of the data (denoted by M) is always assumed to be larger than the number of the normal and orthogonal functions (denoted by N).

Now the inverse problem is reduced to that of finding the vector $\boldsymbol{B}$ from Eq. (12). It is a typical linear inverse problem with discrete data. In principle, by use of singular value decomposition (SVD), the real coefficient matrix $\boldsymbol{A}_{\mathrm{r}}$ can be decomposed into three matrices,

$$\boldsymbol{A}_{\mathrm{r}} = \boldsymbol{U}\Sigma\boldsymbol{V}^{\mathrm{T}}, \tag{14}$$

where $\boldsymbol{U}$ and $\boldsymbol{V}$ are orthogonal matrices, and Σ is diagonal matrix whose elements are called singular values of the matrix $\boldsymbol{A}_{\mathrm{r}}$. Then one can obtain a least square solution of Eq. (12), which can be written as

$$\boldsymbol{B} = \boldsymbol{V}\Sigma^{-1}\boldsymbol{U}^{\mathrm{T}}\boldsymbol{D}_{\mathrm{r}}. \tag{15}$$

In practice, the singular values of the matrix $\boldsymbol{A}$ tend rapidly to zero, so Eq. (11) is ill-posed and the solution given by Formula (14) is unstable. In this case, we can use the regularized method to get a stable solution of Eq. (11). A special kind of regularized solutions can be written as

$$\boldsymbol{B} = \boldsymbol{V}\boldsymbol{S}^{-1}\boldsymbol{U}^{\mathrm{T}}\boldsymbol{D}, \tag{16}$$

where

$$\boldsymbol{S}^{-1} = [\Sigma + \mu\Sigma^{-1}]^{-1}, \tag{17}$$

and μ is a Lagrange multiplier (also-called regularization parameter) that acts as a trade-off parameter. Establishing a proper way to make choice of the regularization parameter is a key step in dealing with regularized problems and, in this respect, several methods have been reported[7~9]. Here we use an error function that was presented in Ref. [9] to find a proper regularization parameter μ. The error function is defined as

$$\mathrm{ER}(\mu)\ \frac{\sum_{j=1}^{M} = \left| T^{l}(0,\omega_j,\mu) - T_d(\omega_j) \right|^2}{\sum_{i=1}^{M} \left| T_d(\omega_{ji}) \right|^2}, \tag{18}$$

where $T^{l}(0,\omega_j,\mu)$ is the calculated surface temperature in the *l-th* iterative procedure with thermal parameter $\kappa^{l}(z,\mu)$ for a given regularization parameter μ. It can be proven that there exists a minimal value of the function $\mathrm{ER}(\mu)$, while μ has a proper value which is what we want to find out.

2 Numerical simulations and discussion

In the numerical simulation, the sample's thickness is assumed to be 4×10^3 m, and $\rho_c = \rho c = 3.45 \times 10^6$ J deg^{-1} m^{-3}. The surface temperature $T_d(\omega_i)$ which is assumed as the detected signal is calculated from Eqs. (1a) and (1b). The frequency range is set from 1 Hz to higher than 1 MHz. It must be emphasized that the normalized and orthogonal function set $\{\phi_k(z)\}$ used for the expansion of $\delta\kappa^{l}(z)$ in Eq. (7) are Fourier functions, which is very important for the reconstruction of a step function $\kappa(z)$. The inverse procedure of the numerical experiments for the reconstruction of depth distribution $\kappa(z)$ is described as follows: (i) An initial profile distribution $\kappa^{0}(z)$ is assumed firstly. The temperature field $T^{0}(z,\omega)$ is calculated using a layer-built model, then the matrices $\boldsymbol{A}_{\mathrm{r}}$ and $\boldsymbol{D}_{\mathrm{r}}$ can be obtained. (ii) the linear algebraic Eq. (12) is solved using the regularization method for getting the coefficient matrix $\boldsymbol{B}$. The $\delta\kappa^{0}(z)$ is determined by Eq. (8) and then, the first iterative process $\kappa^{1}(z) = \kappa^{0}(z) + \delta\kappa^{0}(z)$ is yielded. (iii) The norm

$$\int_0^L [\kappa^{l+1}(z) - \kappa^{l}(z)]^2 \mathrm{d}z < \varepsilon \tag{19}$$

can be used as a criterion for evaluating the performance of the numerical algorithm. If the desired accuracy is not met, then one can repeat the above steps until the desired accuracy is attained.

The curves shown in Fig. 1 display the reconstructed depth profiles of the thermal conductivity $\kappa(z)$ of assumed samples with various defects. The good agreement of the reconstructed $\kappa(z)$ profiles with original ones demonstrates the reliability and the adaptability of the algorithm. We can see that the reconstructed data roughly indicate the locations and properties of different defects in treated samples.

In order to obtain more information about defects in samples, the reconstructed data can be processed using a simple and effective method, which is described by the following formula:

$$\kappa_j^* = \begin{cases} \kappa_0 & \dfrac{|\kappa_j - \kappa_0|}{|\kappa_{\max} - \kappa_0|} < \dfrac{P}{e} \\[2ex] \kappa_j & \dfrac{|\kappa_j - \kappa_0|}{|\kappa_{\max} - \kappa_0|} \geqslant \dfrac{P}{e} \end{cases}, \qquad \kappa_j \in \{\kappa_i\}, \quad \kappa_j^* \in \{\kappa_i^*\}, \tag{20}$$

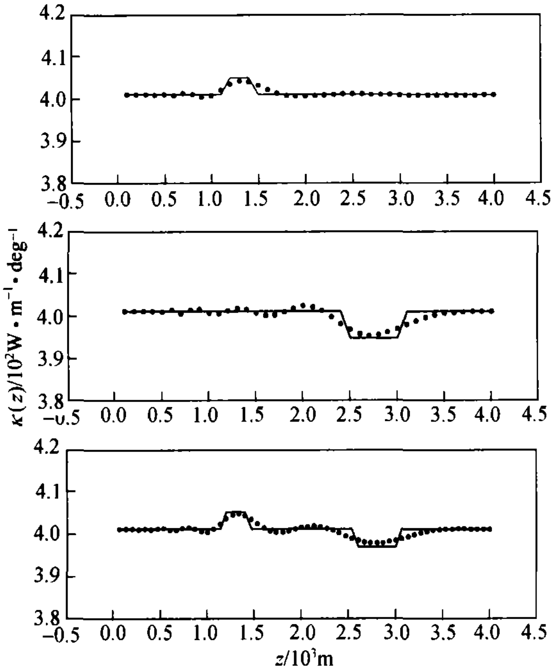

Fig. 1 Reconstructed depth distributions of the thermal conductivity of samples with various defects. The solid lines denote the original $\kappa(z)$, and the dots denote the reconstructed ones.

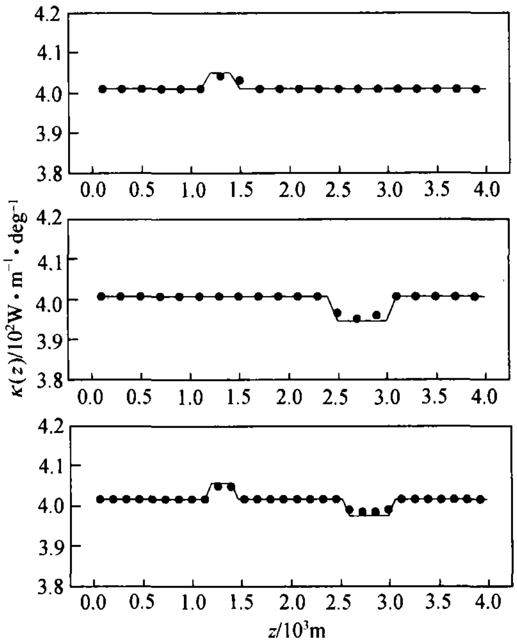

Fig. 2 Depth distribution curves of the thermal conductivity. The solid lines denote the original $\kappa(z)$, and the dots are plotted using the processed data based on the reconstructed ones shown in Figure. 1.

where $\{\kappa_j\}$ denote a series of reconstructed data, $\{\kappa_j^*\}$ the processed data series, κ_0 is the thermal conductivity in the defect free area (the normal area) of the investigated sample which can be taken as a determined constant, $\kappa_{\max} \in \{\kappa_j\}$ makes the absolute value $|\kappa_{\max} - \kappa_0|$ maximized, and P is an experimental constant set at 1.65 for our numerical simulation. The curves in Fig. 2 demonstrate the effect of data processing, from which we know that the location and width of each defect in the treated samples can be precisely determined.

Numerically simulated thermal wave images of a sample with two defects are shown in Fig. 3. The locations and widths of both defects in the sample are clearly displayed with black-white contrast graphs based on the reconstructed data from all the scan points along the sample's surface. We can see that the algorithm of inversion is very effective and suitable for making thermal wave imaging for solid materials.

In practical experiment, the detected surface signals are always mingled with noises. To confirm the performance of the algorithm under noisy condition, we also simulate surface signals with noise to reconstruct the profile of $\kappa(z)$. The surface temperatures mixed with noise can be written as

$$T_{\eta d}(\omega) = T(\omega)(1 + \eta \times RND), \tag{21}$$

where RND is a set of white noise and η is the noise intensity. The thermal graphs shown in Fig. 4 display the thermal imaging effect with noise disturbance, which indicates that this algorithm is still stable and effective as the noise ratio is not larger than 5%.

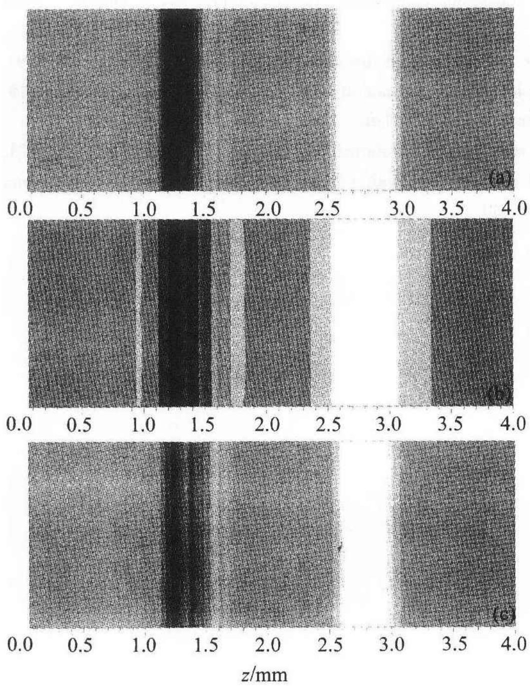

Fig. 3. Thermal wave imaging of an assumed sample with two defects. (a) White-black contrast graph displaying the original distributions of $\kappa(z)$; (b) the graph plotted using reconstructed data directly; (c) the graph plotted using processed data.

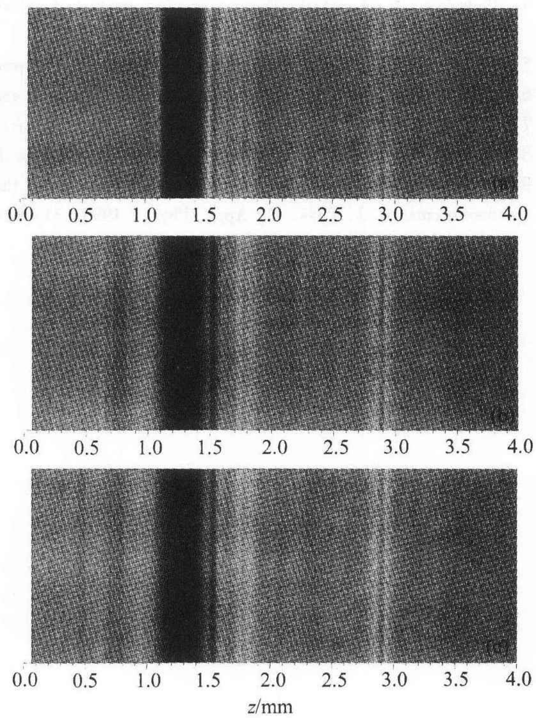

Fig. 4. Thermal wave imaging for an assumed sample with one defect under the condition of noise disturbance. (a) The graph plotted using original data; (b) the graph plotted using reconstructed data from the surface signal with 1% noises; (c) with 5% noises.

3 Conclusions

An iterative method of inversion for the defect in depth evaluation and the thermal wave imaging of solid samples has been discussed. Using the inverse algorithm with the suggested simple and effective data processing method, one can determine precisely the location, width and thermal property of each defect in the investigated sample. The results of numerical simulation indicate that the algorithm of inversion is also effective as the surface temperature signals are mixed with noise, demonstrating the stability and reliability of the algorithm. It should be emphasized that the reconstruction of the defect shape and the thermal property is automatic and does not require any prior information about the detected defects. We want to point out that the algorithm used in this paper is suitable to defect evaluation and thermal wave imaging for samples with layer defects or for layer-built materials. As to a sample with defects limited in geometrical size, one must develop a high dimensional inverse algorithm.

References

1 Mandelis, A. et al. Photothermal wave imaging of metal-oxide-semiconductor field-effect transistor structures. J. Appl. Phys., 1988, 63: 92.

2 Han, X. Y. et al. Quantitative thermal wave imaging of corrosion on aircraft. Review of Progress in QNDE, 1997, 16: 353.

3 Busse, G. et al. Thermal wave imaging with phase sensitive modulated thermography. J. Appl. Phys., 1992, 71: 3962.

4 Plotnikov, Y. A. et al. Thermal graphic imaging of defects in anisotropic composites. Review of Progress in QNDE., 1998, 17: 457.

5 Cheng, J. C. et al. A numerical algorithm for inverse problems in photothermal detection. J. Physique, 1994, 4: C7-559.

6 Cheng, Y. M. et al. A numerical algorithm for remote sensing of thermal conductivity. J. Comput. Phys., 1981, 43: 315.

7 Locker, J. et al. Regularization with differential operator: general theory. J. Math. Anal. Appl., 1980, 74: 504.

8 Bertero, M. et al. Linear inverse problems with discrete data: stability and regularization. Inverse Problems, 1988, 4: 573.

9 Xu, M. H. et al. A new method of reconstruction of thermal conductivity-depth profiles from photoacoustic or photothermal measurements. J. Phys. D: Appl. Phys., 1998, 31: 1.